sensors

MDPI

*Review*

# Screening Genotoxicity Chemistry with Microfluidic Electrochemiluminescent Arrays

**Itti Bist [1], Kiran Bano [1] and James F. Rusling [1,2,3,4,*]**

[1] Department of Chemistry, University of Connecticut, Storrs, CT 06269, USA; Itti.bist@Uconn.edu (I.B.); kiran.bano@uconn.edu (K.B.)
[2] Department of Surgery and Neag Cancer Center, University of Connecticut Health Center, Farmington, CT 06032, USA
[3] Institute of Material Science, University of Connecticut, Storrs, CT 06269, USA
[4] School of Chemistry, National University of Ireland at Galway, Galway, Ireland
* Correspondence: james.rusling@uconn.edu

Academic Editor: María Jesús Lobo-Castañón
Received: 7 April 2017; Accepted: 26 April 2017; Published: 3 May 2017

**Abstract:** This review describes progress in the development of electrochemiluminescent (ECL) arrays aimed at sensing DNA damage to identify genotoxic chemistry related to reactive metabolites. *Genotoxicity* refers to chemical or photochemical processes that damage DNA with toxic consequences. Our arrays feature DNA/enzyme films that form reactive metabolites of test chemicals that can subsequently react with DNA, thus enabling prediction of genotoxic chemical reactions. These high-throughput ECL arrays incorporating representative cohorts of human metabolic enzymes provide a platform for determining chemical toxicity profiles of new drug and environmental chemical candidates. The arrays can be designed to identify enzymes and enzyme cascades that produce the reactive metabolites. We also describe ECL arrays that detect oxidative DNA damage caused by metabolite-mediated reactive oxygen species. These approaches provide valuable high-throughput tools to complement modern toxicity bioassays and provide a more complete toxicity prediction for drug and chemical product development.

**Keywords:** electrochemiluminescence; genotoxicity; arrays; cytochrome P450; microfluidics

## 1. Introduction

Toxic chemicals and their metabolites generated by cytochrome P450 (cyt P450) enzymes and bioconjugate enzymes can cause DNA damage. Various types of DNA damage can be caused by toxic compounds, including oxidation of DNA bases, nucleobase adduct formation, depurination of adducts, and strand breaks [1]. DNA oxidations can occur from ionizing radiation and reactive oxygen species (ROS) [2–4] with the major product 8-oxo-2-deoxyguanosine (8-oxodG) on DNA [5] being responsible for mutagenesis. DNA adducts formed by coupling of reactive metabolites and DNA bases are major biomarkers for cancer risk in humans, so a thorough understanding of reactive metabolites of chemicals generated by cyt P450s [6] and bioconjugation enzymes is essential for a complete toxicity pathway assessment of chemicals and drugs.

Electrochemical methods for DNA damage and toxicity detection were pioneered by Paleček [7] and Fojta [8]. To date, various electrochemical sensors for DNA damage, DNA interactions with drugs, environmental pollutants, and other potentially genotoxic species have been developed and reviewed by various authors [9–14]. However, our group is the only one to develop metabolite-generating microfluidic electrochemiluminescent (ECL) arrays for predicting metabolic genotoxicity chemistry of xenobiotics. This review focuses on our ECL sensor technology for genotoxicity screening.

Our approach as described herein features ECL arrays comprised of microwells containing dense DNA/enzyme films that produce metabolites in close proximity to DNA. ECL dyes that utilize damaged DNA as a co-reactant are included in the microwells. Extension of reactive metabolite studies to complementary LC-MS/MS analyses can be done utilizing DNA/enzyme films on magnetic beads to biocolloid enzyme reactors [15–18]. This review describes the sensor arrays, chemistry, and mechanisms of genotoxicity revealed using these ECL arrays.

## 2. Metabolic Pathway Involved in Genotoxicity

Cyt P450s are important metabolic enzymes that catalyze 75% of all known metabolic reactions involving drugs and other xenobiotics and can often generate reactive metabolites [19,20]. These reactive metabolites can cause DNA damage, and the parent chemicals are then described as *genotoxic*. Cyt P450-catalyzed metabolic pathways works through a complex catalytic cycle by involving the ferric iron–heme (P-Fe) prosthetic group. A two-electron reduction of the heme iron breaks the oxygen-$Fe^{III}$ bond using electrons shuttled by cyt P450 reductase (CPR) from NADPH to cyt P450s. Reduction of cyt P450-$Fe^{III}$ and protonation yields the cyt P450-$Fe^{III}$-hydroperoxo complex **6** (Scheme 1). This complex then produces an active ferryloxy species (cyt P450-$Fe^{IV}$=O, **7**) that transfers oxygen to bound substrate (RH) to oxidize it, often by an oxygen transfer reaction. The oxidized group can then serve as a site for attaching a solubilizing conjugate. Our genotoxicity assays can incorporate any human cyt P450s and/or metabolic bioconjugation enzymes to mimic these events in the human body [15]. Many substrates yield DNA-reactive metabolites, including styrene, polyaromatic hydrocarbons, nitrosamines, aromatic amines, tamoxifen, and other chemotherapeutic agents [21–24].

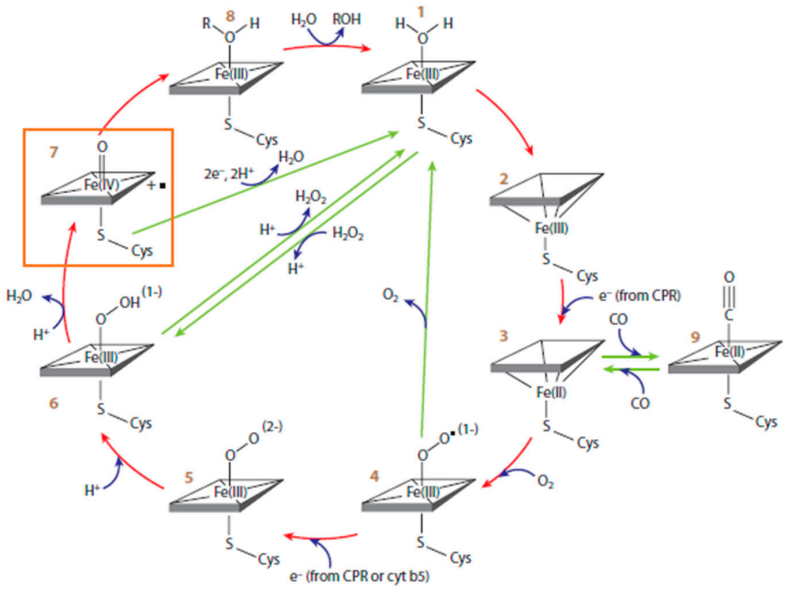


**Scheme 1.** The proposed catalytic pathway for cyt P450-catalyzed metabolic reactions [17,25].

## 3. Development of ECL-Based Genotoxicity Sensors

Our early toxicity sensors combined metabolic enzymes, DNA, and polyions in layer-by-layer (LBL) thin films on graphite electrodes through electrostatic adsorption of alternately charged layers of a redox ECL polymer, DNA, enzymes, and synthetic polyions [26]. Metabolites are produced in an enzyme reaction step, and DNA damage is subsequently monitored using ECL and LC-MS bioreactors [27,28]. The ECL dye polycation (bis-2,2′-bipyridyl) ruthenium polyvinylpyridine ($[Ru(bpy)_2(PVP)_{10}]^{2+}$ or RuPVP) is oxidized by the electrode at ~1.2 V vs. Ag/AgCl to yield $Ru^{III}$-PVP, which catalytically oxidizes guanines to guanine radicals (G•). G• in intact DNA serves as an ECL co-reactant to eventually

produce excited $Ru^{2+}$*-PVP, which emits light at 610 nm (Scheme 2). Initially, single electrode ECL sensors coated with RuPVP/enzyme/DNA were developed as shown in Scheme 3A. These sensors in some cases measured ECL and voltammetry simultaneously [29,30].

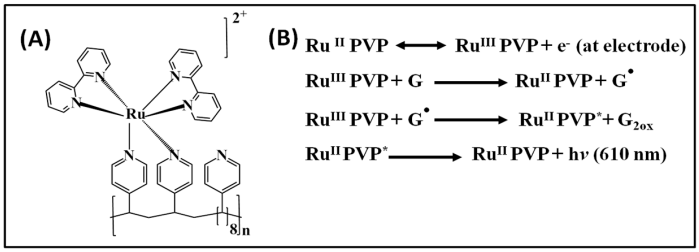


**Scheme 2.** (**A**) Structure of ruthenium polyvinylpyridine (RuPVP); (**B**) proposed reaction mechanism for electrochemiluminescent (ECL) generation using RuPVP and guanines in DNA.

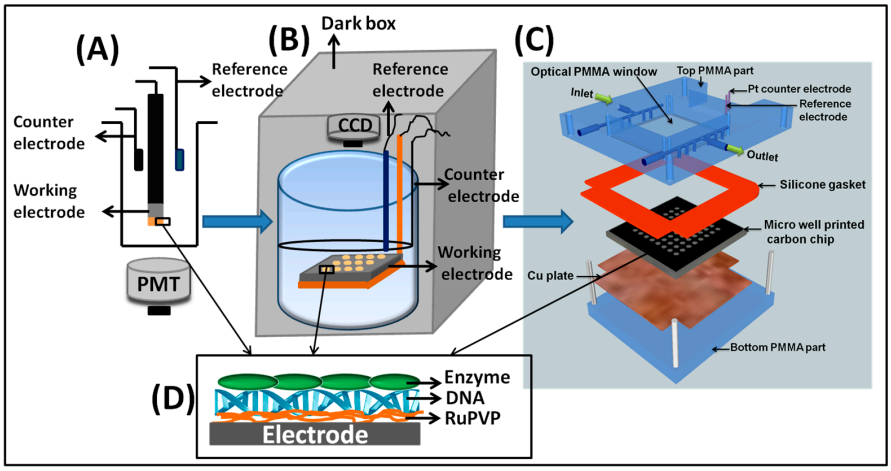


**Scheme 3.** Evolution of ECL genotoxicity sensors, starting from a single sensor to a 64-microwell array. (**A**) A single-electrode sensor coated with RuPVP/enzyme/DNA films as shown in (**D**). The sensor was placed above an optical fiber connected to a photomultiplier tube (PMT) for ECL detection. (**B**) Array showing a pyrolytic graphite (PG) chip working electrode with the RuPVP/enzyme/DNA film spots shown with Ag/AgCl reference and Pt-ring wire counter electrode. After the enzyme reaction driven by NADPH, for ECL readout, the device is placed in a dark box and 1.2 V are applied while a charge-coupled device (CCD) camera measures ECL. (**C**) Recent ECL microwell PG chip in a microfluidic reaction chamber with symmetrically placed reference and counter electrodes on the underside of the top plate. Reactants flow into the chamber, and ECL is then captured by using a CCD camera in a dark box.

We also demonstrated ECL from oxidized DNA in ultrathin films of cationic polymer $[Os(bpy)_2(PVP)_{10}]^{2+}$ [PVP = poly(vinyl pyridine)] or OsPVP utilizing 8-oxodG as the co-reactant [31]. OsPVP combined with RuPVP were assembled into films with DNA or oligonucleotides to detect both DNA oxidation and nucleobase adducts from chemical damage. Electrochemically oxidized $Os^{II}$ sites were generated from films containing 8-oxodG on DNA formed by chemical oxidation using a Fenton reagent that produced ECL specific for oxidized DNA, and $Ru^{II}$ sites gave ECL from chemically damaged DNA, and possibly from cleaved DNA strands [28].

More recently, we have incorporated microsomal CPR/cyt P450 films on electrodes to mimic the situation in vivo. Cyclic voltammetry (CV) of this system closely mimics the details of the natural cyt P450 catalytic pathway. As in Scheme 1, electrons flow from the electrode to CPR and then to the cyt P450 as in the in vivo pathway to facilitate efficient catalytic turnover of the cyt P450s [32]. CPR is reduced by the electrode but cyt P450s are not (Scheme 4, Equation (1)). $CPR_{red}$ exists in redox

equilibrium with cyt P450$Fe^{III}$ to yield $CPR_{ox}$ as a product (Scheme 4, Equation (2)), and electrochemical oxidation of $CPR_{red}$ (Scheme 4, Equation (3)) competes with this equilibrium. We later found that a similar catalytic mechanism can be activated in microsomes containing multiple cyt P450s and CPRs [26,33,34]. Thus, the microsomal CPR-containing film is a model for the natural cyt P450 catalysis pathway [30] and can be used in toxicity sensors to electrochemically active cyt P450s.

Catalytic oxidation of 4-(Methylnitrosamino)-1-(3-pyridyl)-1-butanone (NNK) with the CPR/cyt P450 films further confirmed the electrode CPR cyt P450 pathway for activation of cyt P450s [32,33]. The formation rate of the product of this reaction in bulk electrolysis was slightly larger than that achieved in the same system using NADPH as electron donor. CV simulations (Scheme 4, Equation (1)) suggest an equilibrium complex between CPR and cyt P450 that facilitates electron transfer [35]. The theoretical data ($k_b \geq 5k_f$ and $K = k_f/k_b \leq 0.2$, where $k_f$ and $k_b$ are forward and backward second-order chemical rate constants and $K$ is the equilibrium constant) lies in favor of $CPR_{red}$, which is why $CPR_{ox}$ is reduced electrochemically in cyt P450/CPR films that are preferential to cyt P450. The difference in formal potential ($\Delta E^\circ$) between CPR and cyt P450 is $\Delta E^\circ = [RT/nF] \ln(K)$, where $R$ is the gas constant, $T$ is the absolute temperature, and $F$ is Faraday's constant. Thus, $K < 0.2$ predicts that cyt P450 formal potential is ~40 mV negative of $CPR_{ox}$ in the films, so that $CPR_{ox}$ is more easily reduced. $O_2$ present in catalytic oxidations reacts with P450-$Fe^{II}$ and the equilibrium shifts to the right to drive substrate oxidation [32].

$$\mathbf{CPR_{ox} + e \longrightarrow CPR_{red} \quad E^{\circ\prime} = -230\ mV\ vs.\ NHE;\ k_{s,red} = 0.4\ s^{-1}} \qquad (1)$$

$$\mathbf{CPR_{red} + cyt\ P450\text{-}Fe^{III} \rightleftharpoons CPR_{ox} + cyt\ P450\text{-}Fe^{II}\ k_b \geq 5k_f} \qquad (2)$$

$$\mathbf{CPR_{red} - e \longrightarrow CPR_{ox} \quad E^{\circ\prime} = -230\ mV\ vs.\ NHE;\ k_{s,ox} = 40\ s^{-1}} \qquad (3)$$

**Scheme 4.** $E_rCE_o$ simulation model for cyclic voltammetry (CV) of cyt P450s + cyt P450 reductase (CPR).

## 4. Microfluidic ECL Arrays for Genotoxicity Screening

ECL-based genotoxicity sensor arrays were first developed in our laboratory in 2007. These arrays were fabricated on a single conductive chip instead of multielectrode devices. In these ECL arrays, a 1-$inch^2$ (6.45 $cm^2$) pyrolytic graphite (PG) block was electrically connected to a copper block via silver epoxy and insulated using ethyl acrylate so only the upper conductive PG face was exposed. RuPVP/enzyme/DNA films were spotted on demarcated locations. Metabolite generation was driven by manual deposition and incubation of reactants on the arrays (Scheme 3B), using an NADPH regeneration system to drive cyt P450 catalysis.

These ECL arrays eventually led to our current high-throughput arrays integrated into a microfluidic reactor. A 64-microwell pattern was computer laser-jet printed and transferred onto a cleaned and polished PG chip (2.5 × 2.5 × 0.3 cm) by heat pressing the mask onto the PG chip at 290 °F (143 °C) for 90 s. The hydrophobic toner separating the spots prevents cross-contamination of DNA, enzyme and polymer solutions deposited in each well for LBL film formation. Individual RuPVP/enzyme/DNA spots were constructed in each microwell by sequential depositions of 1 µL drops of the appropriate solution. Then, the PG chip was fitted into a microfluidic reaction cell consisting of top and bottom poly(methylmethacrylate) (PMMA) plates with an optical glass window to facilitate ECL light acquisition. Pt counter and Ag/AgCl reference electrode wires were fixed on the bottom side of the top PMMA plate. A silicone rubber gasket sandwiched between the PMMA plates was used to form a sealed channel, and a copper plate was placed underneath the PG chip for electrical connection. The microfluidic device was connected to a syringe pump for a constant flow of reactants or buffers at a fixed concentration and flow rate to better control reaction conditions in the semi-automated system (Scheme 3C). Metabolites were generated in situ by flowing test compounds through the chip, and ECL was then generated by applying a potential of 1.25 V vs. Ag/AgCl for 180 s and captured by a CCD camera in a dark box.

Our first task for this microfluidic reactor focused on reactive metabolites of benzo[a]pyrene (B[a]P). Cyt P450 enzyme sources included rat liver microsomes (RLM) and human liver microsomes (HLM), supersomes (genetically engineered to contain only one cyt P450 + CPR) of cyt 1B1, 1A1, and 1A2 and human liver S9 fraction. B[a]P was initially oxidized by cyt P450s to B[a]P-7,8-epoxide (Scheme 5, Equation (1)), which was then hydrolyzed to B[a]P-7,8-dihydrodiol in presence of epoxide hydrolase (EH, Equation (2)). Further oxidation of dihydrodiol by cyt P450 resulted in the formation of reactive metabolite B[a]P-7,8-dihydrodiol-9,10-epoxide (BPDE, Equation (3)), which reacts with guanine and adenine bases in DNA to form adducts.

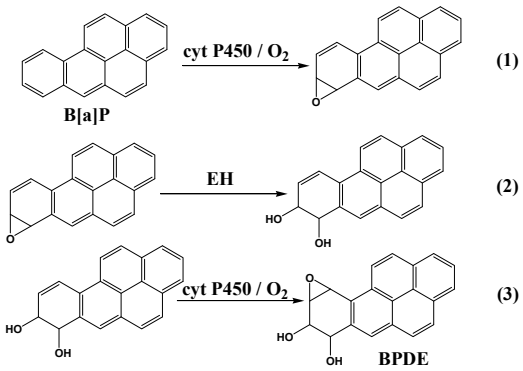


**Scheme 5.** Metabolic activation of B[a]P by cyt P450 and epoxide hydrolase (EH).

ECL is normalized for the amount of enzyme in each film (estimated by quartz crystal microbalance) to find the relative rate of DNA damage by B[a]P metabolites. The relative rate of DNA damage was higher when EH was included with cyt P450 in microwells when using HLM, RLM, or supersomes, suggesting a complete bioactivation of B[a]P to produce DNA-BPDE adducts. Cyt P450 1B1 was found to have the highest rate of DNA damage followed by cyt P450s 1A1 and 1A2 (Figure 1). The formation of DNA adducts in the presence of B[a]P was confirmed by liquid chromatography–mass spectrometry (LC-MS/MS) by determining dG-BPDE and dA-BPDE adducts using similar films of DNA/enzyme on magnetic bead reactors. The ECL arrays can also measure enzyme inhibition, in this case by measuring a decrease in the %ECL corresponding to a decrease in DNA damage, in the presence of furafylline and rhapontigenin, which are known inhibitors of cyt 1A2 and 1A1, respectively [36].

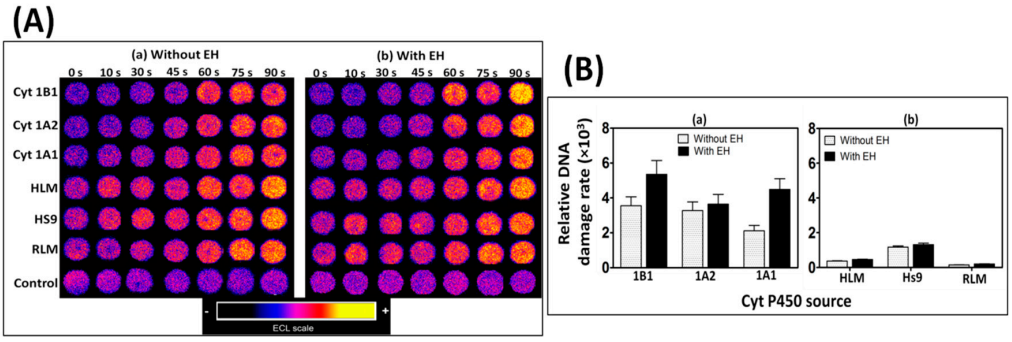


**Figure 1.** (**A**) Recolorized and reconstructed ECL array results for enzyme reactions with oxygenated 25 μM B[a]P + 1% DMSO in pH = 7.4 phosphate buffer with electronic activation of cyt P450s. Microwells containing RuPVP/enzyme/DNA film assemblies exposed to B[a]P for various reaction times. Enzyme sources are cyt P450 supersomes, human, and rat liver microsomes (HLM and RLM), epoxide hydrolase (EH), and human S9 fractions (HS9). (**B**) Influence of EH on the sensor array, relative DNA damage rate for 25 μM B[a]P at pH 7.4: (**a**) supersomes; (**b**) microsomes. Reproduced from [36] with permission, copyright Royal Society of Chemistry, 2013.

## 5. ECL Arrays for Assessing Organ-Specific Metabolic Toxicity

Traditional toxicity assessment focuses on the liver, however, extra-hepatic tissues are also capable of metabolizing xenobiotics into reactive metabolites. The 64-microwell ECL array described above was further developed to evaluate possible genotoxic chemistry effect with different organ enzymes. Enzymes from human liver, lung, intestine, and kidney were compared in the array (Scheme 6).

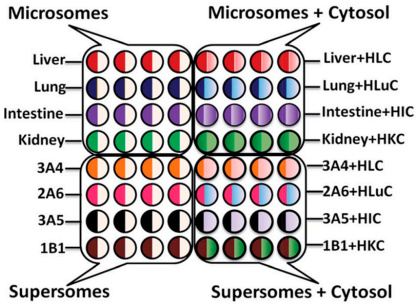


**Scheme 6.** Experimental design of 64-microwell ECL chip with films of RuPVP/enzymes/DNA for metabolic genotoxicity assays of test compounds. Symbols: H = human; L = liver; C = cytosol; Lu = lung; I = intestine; K = kidney; numbers and letters such as 3A4 indicate supersomes containing the denoted single cyt P450 manifold. Reproduced from [37] with permission, copyright Royal Society of Chemistry, 2015.

4-(Methylnitrosamino)-1-(3-pyridyl)-1-butanone (NNK), a known carcinogen, was used as a test compound to study the organ-specific metabolic-DNA reactions for enzymes from the different organs (Figure 2). A decrease in relative DNA damage rates in the presence of cytosolic enzymes and their co-factors were observed, which is consistent with the detoxification effect of cytosols via various bioconjugation pathways [37].

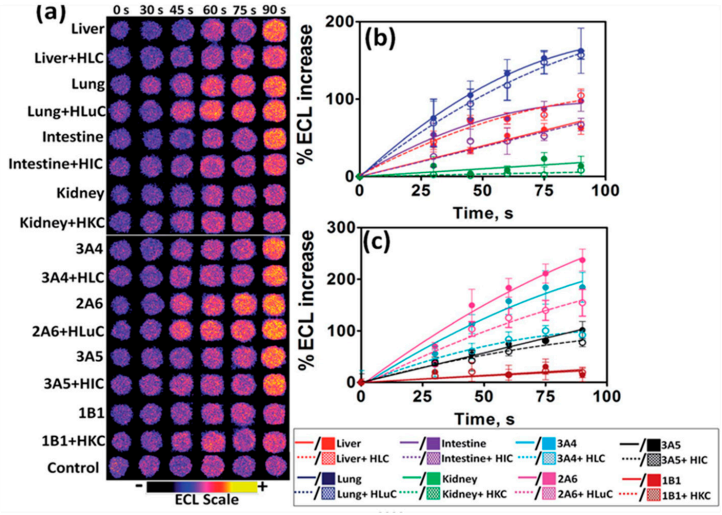


**Figure 2.** ECL results from genotoxicity study of oxygenated 150 μM NNK in pH 7.4 phosphate buffer and necessary cofactors exposed to microwells containing RuPVP/enzyme/DNA with electrochemical activation of cyt P450s at −0.65 V vs. Ag/AgCl (0.14 M KCl) for different reaction times. (**a**) Reconstructed, recolorized ECL array images. Control spots contain microsomes exposed to the same reaction conditions as above without exposure to NNK. Graphs show influence of enzyme reaction time on %ECL increase for reaction with 150 μM NNK at pH = 7.4, (**b**) with human organ tissue enzymes, and (**c**) with individual cyt P450 supersomes. Reproduced from [37] with permission, copyright Royal Society of Chemistry, 2015.

The two-tier approach based on ECL array and LC-MS/MS biocolloid reactors provided a more detailed profile of possible genotoxicity pathways associated with specific organs. Correlations between DNA damage rates obtained from the cell-free ECL arrays and cell-based Comet assays that measure DNA damage in cells were found [37].

## 6. ECL Sensor Arrays for DNA Oxidation

Oxidative stress or oxidative DNA damage is an imbalance between the production of ROS and the ability of the body to counteract their harmful effects [38]. ROS oxidizes guanosines (dG) in the DNA to form 8-oxodG, a biomarker for oxidative DNA damage [39]. 8-OxodG serves as a co-reactant for Osmium complex $[Os(bpy)_2(phen\text{-}benz\text{-}COOH)]^{2+}$ {bpy = 2,2′-bipyridine; phen-benz-COOH = (4(1,1phenanthrolin-6-yl)benzoic acid)}. ECL is generated due to selective catalytic oxidation of 8-oxodG by $Os^{III}$ sites in the polymer, leading to the formation of a photoexcited $Os^{II*}$ species that emits ECL [31]. The 64-microwell array described in the above section was used to develop an ECL array for oxidative DNA damage.

8-oxodG was detected in intact ds-DNA using composite films of $[Os(bpy)_2(phen\text{-}benz\text{-}COOH)]^{2+}$ (Scheme 7), Nafion polymer, and reduced graphene oxide (OsNG) [40]. A homogeneous solution of $[Os(bpy)_2(phen\text{-}benz\text{-}COOH)]^{2+}$-Nafion was drop-casted into the microwells of the PG chip array containing a layer of reduced graphene oxide, followed by the deposition of oxidized DNA solution on the OsNG-modified films. The PG chip is placed in the microfluidic device and washed, and ECL is then captured using a CCD camera while applying 0.9 V vs. Ag/AgCl. Fenton's reagent was used as a model compound for DNA and polydeoxyguanosine (polyG) oxidation, and an increase in the ECL with the increase in the reaction time was observed (Figure 3).

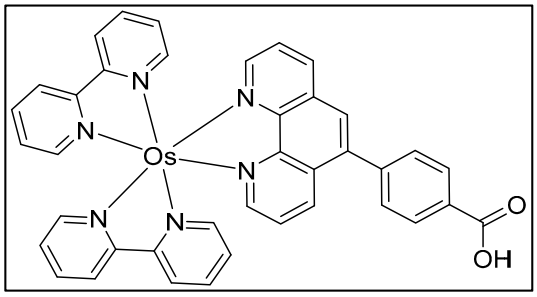


**Scheme 7.** Structure of $[Os(bpy)_2(phen\text{-}benz\text{-}COOH)]^{2+}$.

For array standardization, the amount of 8-oxodG in DNA oxidized by Fenton's reagent was measured using UHPLC-MS/MS. The ratio of 8-oxodG to the total amount of dG increased with the oxidation time in the UHPLC-MS/MS experiments, which was used to obtain relative amounts of 8-oxodG. A calibration curve of %ECL increase vs. relative 8-oxodG concentration from UHPLC-MS/MS was used to quantitate 8-oxodG in the array (Figure 3d,e). The array was also used to measure metabolite-mediated DNA oxidation. This ECL array enabled 64 experiments in one run and only 1 μg of the DNA is required to perform an experiment. The detection limit was 1500 8-oxodG per $10^6$ nucleobases [40].

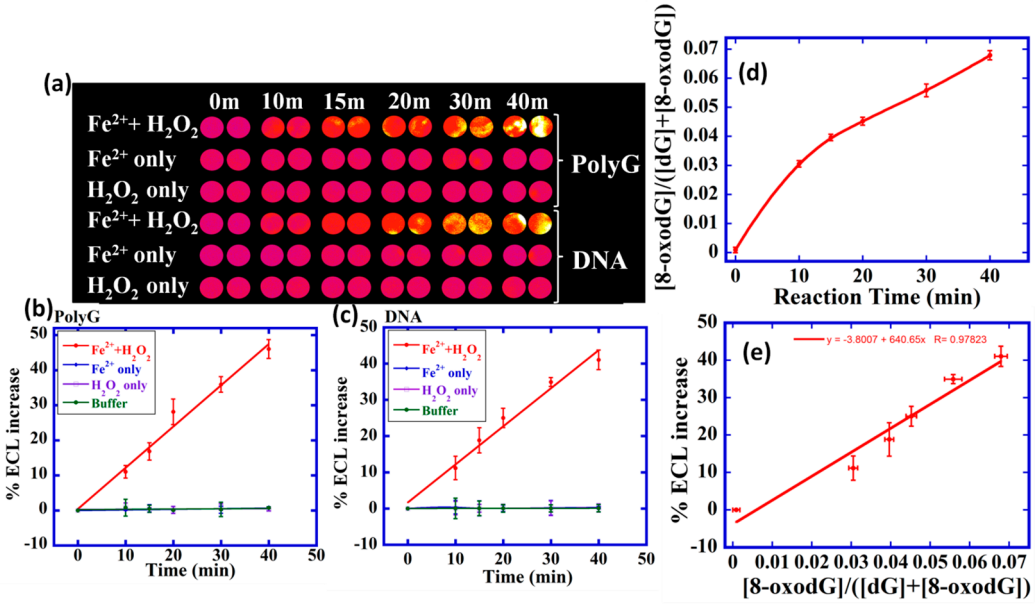


**Figure 3.** ECL array data for polyG and DNA oxidation. (**a**) Reconstructed ECL array data demonstrating ECL from spots of OsNG/polyG or DNA film treated with Fenton's reagent in pH 7.2 phosphate buffer saline for various time intervals. Controls are polynucleotides treated only with buffer, with only $FeSO_4$ or with only $H_2O_2$. Graphs show relative %ECL increase for (**b**) polyG and (**c**) DNA. (**d**) UHPLC-MS/MS for ECL array calibration showing measured ratio of [8-oxodG]/([dG]+[8-oxodG]) for DNA reacted with Fenton's reagent for different time and then hydrolyzed. (**e**) Calibration plot for %ECL increase vs. relative amount of 8-oxodG. Reprinted with permission from [40], copyright (2016), American Chemical Society.

## 7. Summary and Conclusions

It is clear that multiple in vitro toxicity screening tools are needed to approach reliable predictions of in vivo toxicity risks. Our two-tiered approach of ECL microfluidic array and LC-MS/MS biocolloid reactors can provide detailed information on possible pathways of genotoxicity that are not forthcoming from bioassays, but are important components of a toxicity assessment. Microfluidic ECL arrays using RuPVP/DNA/enzyme films detect relative rates of DNA adduct damage from reactive metabolites. $[Os(bpy)_2(phen\text{-}benz\text{-}COOH)]^{2+}$ detects DNA oxidation. LC-MS/MS elucidates structures and measures the formation rates of individual nucleobase adducts and can also detect the amounts of 8-oxodG formed. Molecular pathway information obtained by these approaches can be integrated with other bioassays to provide better future predictions of genotoxicity of chemical and drug candidates.

**Acknowledgments:** The work described herein and the preparation of this article were supported financially by the National Institute of Environmental Health Sciences (NIEHS), NIH, USA. Grant ES03154. The authors thank the coworkers and collaborators named in joint publications for their many excellent contributions to this research, without which progress would not have been possible.

**Conflicts of Interest:** The authors declare no conflict of interest.

## References

1. Nassar, A.; Hollenburg, P.F.; Scatina, J. *Drug Metabolism Handbook: Concepts and Applications*; John Wiley & Sons: Hoboken, NJ, USA, 2009.
2. Halliwell, B.; Gutteridge, M.C. Oxygen toxicity, oxygen radicals, transition metals and disease. *Biochem. J.* **1984**, *219*, 1–14. [CrossRef] [PubMed]
3. Duracková, Z. Some current insights into oxidative stress. *Physiol. Res.* **2010**, *59*, 459–469. [PubMed]

4. Reuter, S.; Gupta, S.C.; Chaturvedi, M.M.; Aggarwal, B.B. Oxidative stress, inflammation, and cancer: How are they linked? *Free Radic. Biol. Med.* **2010**, *49*, 1603–1616. [CrossRef] [PubMed]
5. White, B.; Smyth, M.R.; Stuart, J.D.; Rusling, J.F. Oscillating formation of 8-oxoguanine during DNA oxidation. *J. Am. Chem. Soc.* **2003**, *125*, 6604–6605. [CrossRef] [PubMed]
6. Guengerich, F.P. Common and uncommon cytochrome p450 reactions related to metabolism and chemical toxicity. *Chem. Res. Toxicol.* **2001**, *14*, 611–650. [CrossRef] [PubMed]
7. Paleček, E. Past, present, and future of nucleic acids electrochemistry. *Talanta* **2002**, *56*, 809–819. [CrossRef]
8. Fojta, M. Detecting DNA damage with electrodes. In *Electrochemistry of Nucleic Acids and Proteins*; Paleček, E., Scheller, F., Wang, J., Eds.; Elsevier: Amsterdam, The Netherlands, 2005; Volume 1, pp. 386–482.
9. Vyskočil, V.; Labuda, J.; Barek, J. Voltammetric detection of damage to DNA caused by nitro derivatives of fluorene using an electrochemical DNA biosensor. *Anal. Bioanal. Chem.* **2010**, *397*, 233–241. [CrossRef] [PubMed]
10. Hájková, A.; Barek, J.; Vyskočil, V. voltammetric determination of 2-aminofluoren-9-one and investigation of its interaction with DNA on a glassy carbon electrode. *Electroanalysis* **2015**, *27*, 101–110. [CrossRef]
11. Horakova, E.; Barek, J.; Vyskocil, V. Voltammetry at a hanging mercury drop electrode as a tool for the study of the interaction of double-stranded DNA with genotoxic 4-nitrobiphenyl. *Electroanalysis* **2016**, *28*, 2760–2770. [CrossRef]
12. Hájková, A.; Barek, J.; Vyskočil, V. Electrochemical DNA biosensor for detection of DNA damage induced by hydroxyl radicals. *Bioelectrochemistry* **2017**, *116*, 1–9. [CrossRef] [PubMed]
13. Fojta, M.; Daňhel, A.; Havran, L.; Vyskočil, V. Recent progress in electrochemical sensors and assays for DNA damage and repair. *Trends Anal. Chem.* **2016**, *79*, 160–167. [CrossRef]
14. Labuda, J.; Vyskocil, V. DNA/electrode interface, detection of damage to DNA using DNA-modified electrodes. In *Encyclopedia of Applied Electrochemistry*; Kreysa, G., Ota, K., Savinell, R.F., Eds.; Springer Science + Business Media: New York, NY, USA, 2014; pp. 346–350.
15. Hvastkovs, E.G.; Rusling, J.F. State-of-the-Art metabolic toxicity screening and pathway evaluation. *Anal. Chem.* **2016**, *88*, 4584–4599. [CrossRef] [PubMed]
16. Rusling, J.F.; Wasalathanthri, D.P.; Schenkman, J.B. Thin multicomponent films for functional enzyme devices and bioreactor particles. *Soft Matter* **2014**, *10*, 8145–8156. [CrossRef] [PubMed]
17. Hvastkovs, E.G.; Schenkman, J.B.; Rusling, J.F. Metabolic toxicity screening using electrochemiluminescence arrays coupled with enzyme−DNA biocolloid reactors and LC−MS. *Annu. Rev. Anal. Chem.* **2012**, *5*, 79–105. [CrossRef] [PubMed]
18. Rusling, J.F.; Hvastkovs, E.G.; Schenkman, J.B. Screening for reactive metabolites using genotoxicity arrays and enzyme/DNA biocolloids. In *Drug Metabolism Handbook: Concepts and Applications*; Nassar, A., Hollenburg, P.F., Scatina, J., Eds.; John Wiley & Sons Inc.: Somerset, NJ, USA, 2009; pp. 307–340.
19. Schenkman, J.B.; Greim, H. *Cytochrome P450*; Springer: Berlin, Germany, 1993.
20. Shimada, T.; Yamazaki, H.; Mimura, M.; Wakamiya, N.; Ueng, Y.F.; Guengerich, F.P.; Inui, Y. Characterization of microsomal cytochrome p450 enzymes involved in the oxidation of xenobiotic chemicals in human fetal liver and adult lungs. *Drug Metab. Dispos.* **1996**, *24*, 515–522. [PubMed]
21. Bond, J.A. Review of the toxicology of styrene. *Crit. Rev. Toxicol.* **1989**, *19*, 227–249. [CrossRef] [PubMed]
22. Umemoto, A.; Komaki, K.; Monden, Y.; Suwa, M.; Kanno, Y.; Kitagawa, M.; Suzuki, M.; Lin, C.X.; Ueyama, Y.; Momen, M.A.; et al. Identification and quantification of tamoxifen-DNA adducts in the liver of rats and mice. *Chem. Res. Toxicol.* **2001**, *14*, 1006–1013. [CrossRef] [PubMed]
23. Pfeifer, G.P.; Denissenko, M.F.; Olivier, M.; Tretyakova, N.; Hecht, S.S.; Hainaut, P. Tobacco smoke carcinogens, DNA damage and p53 mutations in smoking-associated cancers. *Oncogene* **2002**, *21*, 7435–7451. [CrossRef] [PubMed]
24. Cavalieri, E.L.; Rogan, E.G.; Devanesan, P.D.; Cremonesi, P.; Cerny, R.L.; Gross, M.L.; Bodell, W.J. Binding of benzo[a] pyrene to DNA by cytochrome P-450 catalyzed one-electron oxidation in rat liver microsomes and nuclei. *Biochemistry* **1990**, *29*, 4820–4827. [CrossRef] [PubMed]
25. Ortiz de Montellano, P.R. *Cytochrome P450*, 3rd ed.; Springer: New York, NY, USA, 2005.
26. Rusling, J.F.; Hvastkovs, E.G.; Hull, D.O.; Schenkman, J.B. Biochemical applications of ultrathin films of enzymes, polyions and DNA. *Chem. Commun.* **2008**, *2*, 141–154. [CrossRef] [PubMed]
27. Rusling, J.F. Sensors for toxicity of chemicals and oxidative stress based on electrochemical catalytic DNA oxidation. *Biosens. Bioelectron.* **2004**, *20*, 1022–1028. [CrossRef] [PubMed]

28. Rusling, J.F. Sensors for genotoxicity and oxidized DNA. In *Electrochemistry of Nucleic Acids and Proteins*; Paleček, E., Scheller, F., Wang, J., Eds.; Elsevier: Amsterdam, The Netherlands, 2005; Volume 1, pp. 433–450.
29. Dennany, L.; Forster, R.J.; Rusling, J.F. Simultaneous direct electrochemiluminescence and catalytic voltammetry detection of DNA in ultrathin films. *J. Am. Chem. Soc.* **2003**, *125*, 5213–5218. [CrossRef] [PubMed]
30. So, M.; Hvastkovs, E.G.; Schenkman, J.B.; Rusling, J.F. Electrochemiluminescent/voltammetric toxicity screening sensor using enzyme-generated DNA damage. *Biosens. Bioelectron.* **2007**, *23*, 492–498. [CrossRef] [PubMed]
31. Dennany, L.; Forster, R.J.; White, B.; Smyth, M.; Rusling, J.F. Direct electrochemiluminescence detection of oxidized DNA in ultrathin films containing $[Os(bpy)_2(PVP)_{10}]^{2+}$. *J. Am. Chem. Soc.* **2004**, *126*, 8835–8841. [CrossRef] [PubMed]
32. Krishnan, S.; Wasalathanthri, D.; Zhao, L.; Schenkman, J.B.; Rusling, J.F. Efficient bioelectronic actuation of the natural catalytic pathway of human metabolic cytochrome p450s. *J. Am. Chem. Soc.* **2011**, *133*, 1459–1465. [CrossRef] [PubMed]
33. Krishnan, S.; Hvastkovs, E.G.; Bajrami, B.; Schenkman, J.B.; Rusling, J.F. Metabolic toxicity of 4-(methylnitrosamino)-1-(3-pyridyl)-1-butanone (NNK) evaluated using electrochemiluminescent arrays and human cyt p450s. *Mol. Biosyst.* **2009**, *5*, 163–169. [CrossRef] [PubMed]
34. Krishnan, S.; Rusling, J.F. Thin film voltammetry of metabolic enzymes in rat liver microsomes. *Electrochem. Commun.* **2007**, *9*, 2359–2363. [CrossRef] [PubMed]
35. Rusling, J.F.; Forster, R.J. Electrochemical catalysis with redox polymer and polyion-protein films. *J. Colloid Interface Sci.* **2003**, *262*, 1–15. [CrossRef]
36. Wasalathanthri, D.P.; Malla, S.; Bist, I.; Tang, C.K.; Faria, R.C.; Rusling, J.F. High-throughput metabolic genotoxicity screening with a fluidic microwell chip and electrochemiluminescence. *Lab Chip* **2013**, *13*, 4554–4562. [CrossRef] [PubMed]
37. Wasalathanthri, D.P.; Li, D.; Song, D.; Zheng, Z.; Choudhary, D.; Jansson, I.; Lu, X.; Schenkman, J.B.; Rusling, J.F. Elucidating organ-specific metabolic toxicity chemistry from electrochemiluminescent enzyme/DNA arrays and bioreactor bead-LC-MS/MS. *Chem. Sci.* **2015**, *6*, 2457–2468. [CrossRef] [PubMed]
38. Kohen, R.; Nyska, A. Oxidation of biological systems: Oxidative stress phenomena, antioxidants, redox reactions, and methods for their quantification. *Toxicol. Pathol.* **2002**, *30*, 620–650. [CrossRef] [PubMed]
39. Gedik, C.M.; Boyle, S.P.; Wood, S.G.; Vaughan, N.J.; Collins, A.R. Oxidative stress in humans: Validation of biomarkers of DNA damage. *Carcinogenesis* **2002**, *23*, 1441–1446. [CrossRef] [PubMed]
40. Bist, I.; Song, B.; Mosa, I.M.; Keyes, T.E.; Martin, A.; Forster, J.R.; Rusling, J.F. Electrochemiluminescent array to detect oxidative damage in ds-DNA using $[Os(bpy)_2(phen\text{-}benz\text{-}COOH)]^{2+}$/Nafion/Graphene films. *ACS Sens.* **2016**, *1*, 272–278. [CrossRef] [PubMed]